

Detecting Network Instability via Multiscale Detrended Cross-Correlations and MST Topology

Jose De Leon Miranda^a, Marina Dolfin^{a,b,*}, George Kapetanios^a, Leone Leonida^a

^a*King's College London, King's Business School, London, WC2B 4BG, UK*

^b*University of Messina, Department of Engineering, Messina, 98166, IT*

Abstract

We introduce a multiscale measure of network instability based on the joint use of Detrended Cross-Correlation Analysis (DCCA) and Minimum Spanning Tree (MST) filtering. The proposed metric—the *Elastic Detrended Cross-Correlation Ratio* (Elastic DCCR)—is defined as a finite-difference measure of the logarithmic sensitivity of the average MST length to the observation scale. It captures how the structure of cross-correlation networks deforms across different investment horizons. When applied to a network of global equity indices, the Elastic DCCR rises sharply during episodes of financial stress, reflecting increased short-term coordination among investors and a contraction of correlation distances. The measure reveals scale-dependent reconfigurations in network topology that are not visible in single-scale analyses, and highlights clear differences between stressed and stable market regimes. The approach does not assume covariance stationarity and relies only on scale-dependent detrended correlations; as a result, it is broadly applicable to other complex systems in which interaction strength varies with scale.

Keywords: Multiscale networks, Detrended Cross-Correlation Analysis (DCCA), Minimum spanning trees, correlation networks, scaling, network instability

Introduction

Key financial activities—including portfolio construction, risk management, and the pricing of financial instruments—critically depend on the analysis of connectedness among assets and markets [1, 2, 3, 4, 5, 6, 7, 8]. Understanding the structure and temporal evolution of such connectedness is central to identifying regularities and stylized facts in market dynamics. Empirical evidence shows that cross-market correlations fluctuate markedly over time as a result of technological and financial innovations, structural breaks, and changes in global

*Corresponding author

conditions. These fluctuations become especially pronounced during episodes of elevated volatility, when markets display enhanced synchronization [9, 10]. In such regimes, effective dimensionality contracts, liquidity preferences shift, and market participants increasingly coordinate their behaviour across similar horizons [11, 12, 13]. The resulting increase in cross-market coupling amplifies the channels through which shocks propagate, thereby heightening systemic risk [14, 15, 16, 4, 7].

Characterising how the structure of financial networks reorganises across time scales, and how this affects the transmission of risk, remains a central challenge in the study of complex systems. Existing approaches—such as single-scale DCCA estimators or variance-decomposition techniques of Diebold and Yilmaz—capture important features of dependence but do not quantify how the topology of the correlation network itself deforms as the observation scale changes.

The principal contribution of this research is to introduce a scale-comparison metric that detects structural transitions in correlation networks by examining how their topology changes across time horizons. We combine Detrended Cross-Correlation Analysis (DCCA), which measures scale-dependent long-range correlations [17, 18, 19, 20, 21], with the Minimum Spanning Tree (MST), which filters noisy interactions while retaining the essential backbone of the network. We define a new quantity—the Elastic Detrended Cross-Correlation Ratio (Elastic DCCR)—as the finite-difference approximation of the derivative of the logarithmic MST average length with respect to the logarithm of the observation scale. This ratio provides a compact, dimensionless indicator of multiscale topological deformation and serves as a diagnostic of instability: when the network becomes more synchronised at short horizons than at long horizons, the Elastic DCCR exhibits marked deviations from its scale-invariant baseline behaviour.

Our analysis shows that the Elastic DCCR captures periods of structural transition in global equity markets, where investors compress their interactions onto short time scales during episodes of stress. The metric uncovers changes in connectedness that remain hidden to single-horizon analyses, and its behaviour contrasts systematically with the connectedness measures of Diebold and Yilmaz [22]. By combining multiscale cross-correlations with topological filtering, this framework provides a physically interpretable and computationally efficient tool for monitoring systemic change in complex networks. In this sense, the Elastic DCCR plays the role of an order-parameter-like indicator for scale-induced topological transitions in correlation networks.

1. Methods

1.1. Multiscale detrended cross-correlations for network construction

We analyze daily financial market indices and transform the price series $P_i(t)$, with $i = 1, \dots, N$ markets and $t = 1, \dots, T$ observations, into logarithmic returns defined as

$$r_i(t) = \ln P_i(t) - \ln P_i(t-1). \quad (1)$$

To account for volatility clustering and remove heteroskedasticity at the level of each single time series, we filter the returns using a GARCH(1,1) model,

$$r_i(t) = \sigma_i(t) \varepsilon_i(t), \quad (2)$$

and work with the standardized residuals

$$r_{i,f}(t) = \frac{r_i(t)}{\sqrt{h_i(t)}}, \quad (3)$$

where $h_i(t)$ is the conditional variance obtained from the GARCH fit. This step ensures that scale-dependent statistics reflect intrinsic temporal structure rather than volatility bursts.

The filtered series are then normalized to zero mean and unit variance,

$$\tilde{r}_i(t) = \frac{r_{i,f}(t) - \langle r_{i,f} \rangle}{\sigma_{r_i}}, \quad (4)$$

where $\sigma_{r_i} = \sqrt{\langle r_{i,f}^2 \rangle - \langle r_{i,f} \rangle^2}$ and $\langle \cdot \rangle$ denotes a time average over the sample period.

The above standardized returns $\tilde{r}_i(t)$ constitute the inputs for the Detrended Cross-Correlation Analysis (DCCA). The DCCA coefficient quantifies scale-dependent correlation between two non-stationary time series x and y . Given a scale s , the coefficient is defined as

$$\rho_{\text{DCCA}}(s) = \frac{F_{\text{DCCA}}^2(s)}{F_{\text{DFA},x}(s) F_{\text{DFA},y}(s)}, \quad (5)$$

where $F_{\text{DFA},x}(s)$ and $F_{\text{DFA},y}(s)$ are DFA fluctuation functions and $F_{\text{DCCA}}^2(s)$ is the detrended covariance function.

Following the DFA/DCCA framework introduced for a single time series by Peng et al. [23] and generalized by Podobnik and Stanley [17], each time series is integrated to form its cumulative profile,

$$X(t) = \sum_{k=1}^t (x_k - \langle x \rangle), \quad Y(t) = \sum_{k=1}^t (y_k - \langle y \rangle), \quad (6)$$

and partitioned into $N_s = \lfloor T/s \rfloor$ non-overlapping segments of length s . Within each segment of length s , a local polynomial trend is subtracted to obtain the detrended variances

$$f_{\text{DFA},x}^2(n, s) = \frac{1}{s} \sum_{t=1}^s [X(t) - \hat{X}(t)]^2, \quad f_{\text{DFA},y}^2(n, s) = \frac{1}{s} \sum_{t=1}^s [Y(t) - \hat{Y}(t)]^2, \quad (7)$$

and the detrended covariance

$$f_{\text{DCCA}}^2(n, s) = \frac{1}{s} \sum_{t=1}^s [X(t) - \hat{X}(t)][Y(t) - \hat{Y}(t)]. \quad (8)$$

where $\hat{X}(t)$ and $\hat{Y}(t)$ denote the fitted local polynomial trends. Averaging over all segments yields the multiscale fluctuation and covariance functions,

$$F_{\text{DFA},x}(s) = \sqrt{\frac{1}{N_s} \sum_{n=1}^{N_s} f_{\text{DFA},x}^2(n, s)}, \quad F_{\text{DCCA}}^2(s) = \frac{1}{N_s} \sum_{n=1}^{N_s} f_{\text{DCCA}}^2(n, s), \quad (9)$$

which together define $\rho_{\text{DCCA}}(s)$ in Eq. (5).

The DCCA method is well suited for detecting multiscale dependencies, long-range memory, and non-stationary structure in financial and other complex systems [17, 18, 12, 21].

1.2. Average MST length as a multiscale connectivity measure

The DCCA coefficient $\rho_{\text{DCCA}}^{ij}(s)$ is mapped into a correlation-based distance following the geometric construction of Mantegna [24],

$$d_{\text{DCCA}}^{ij}(s) = \sqrt{2 \left[1 - \left(\rho_{\text{DCCA}}^{ij}(s) \right) \right]}, \quad (10)$$

which yields a symmetric, non-negative distance matrix suitable for hierarchical clustering and minimum spanning tree filtering. The transformation is well defined when $|\rho_{\text{DCCA}}^{ij}(s)| \leq 1$; however, strong heterogeneity in long-range dependence (e.g., markedly different Hurst exponents across series) may lead to violations of this condition. In such cases, generalized normalization procedures may be required to ensure distance compatibility for network construction. (see Research Perspectives).

We construct a time- and scale-dependent weighted network with N market indices as nodes and DCCA distances as link weights. For each pair (i, j) , the distance at scale s and time t is

$$d_{\text{DCCA}}^{ij}(s, t) = \sqrt{2 \left[1 - \left(\rho_{\text{DCCA}}^{ij}(s, t) \right) \right]}. \quad (11)$$

The resulting weighted, fully connected network is filtered using the Minimum Spanning Tree (MST) filtering procedure [24, 25, 26, 27].

The MST preserves the strongest connections while eliminating cycles, yielding a sparse backbone that captures the essential topological structure of the underlying correlation network. In our analysis, the MST is constructed using Kruskal's algorithm [28].

To quantify the degree of connectivity in the system at scale s and time t , we compute the *average tree length*,

$$L(s, t) = \frac{1}{N-1} \sum_{(i,j) \in \text{MST}^t} d_{\text{DCCA}}^{ij}(s, t), \quad (12)$$

where the sum runs over the $N-1$ edges of the MST. Shorter values of $L(s, t)$ indicate stronger clustering and tighter interdependence among markets, whereas larger values reflect more weakly connected or more dispersed network structures. [24, 26]. Thus, $L(s, t)$ provides a compact descriptor of the network's multiscale connectivity.

1.3. Scaling structure of the MST topology and Elastic DCCR

Because Detrended Cross-Correlation Analysis yields scale-dependent measures of dependence, the geometry of the corresponding correlation network is also expected to vary with the observation scale. In systems characterised by heterogeneous interaction horizons, such as financial markets with coexisting short- and long-term investors, it is natural to ask whether this scale dependence follows a regular scaling structure.

A convenient summary of network geometry at scale s and time t is provided by the average length of the Minimum Spanning Tree, $L(s, t)$. If correlations reorganise smoothly across horizons, the variation of $L(s, t)$ with respect to s may be approximated locally by a power-law relation,

$$L(s, t) \propto s^{\alpha(t)}, \quad (13)$$

where $\alpha(t)$ is a time-varying scaling exponent. This relation represents a form of local scale invariance in the network topology: small values of $\alpha(t)$ indicate weak sensitivity of connectivity to scale, while larger or rapidly changing values reflect pronounced multiscale heterogeneity. From a network perspective, such behaviour suggests that correlation distances may reorganise in an approximately self-similar manner across observation scales, motivating the exploration of scaling relations for the average MST length.

Under the scaling hypothesis in Eq. (13), the logarithm of the MST length is approximately linear in $\log s$,

$$\log L(s, t) = \alpha(t) \log s + C(t), \quad (14)$$

where $C(t)$ is a slowly varying intercept. Deviations from linearity in log-log space correspond to departures from scale-invariant organisation and signal distortions in the multiscale structure of the correlation network.

Direct estimation of $\alpha(t)$ requires fitting across multiple scales and is therefore sensitive to the choice of scale range, window length, and noise. For monitoring purposes, a simpler and more robust approach is to estimate the local logarithmic sensitivity of $L(s, t)$ using a finite-difference approximation across two representative horizons.

We therefore define the *Elastic Detrended Cross-Correlation Ratio* (Elastic DCCR) as

$$\text{Elastic DCCR}(t) = \frac{\log L(s_{\text{long}}, t) - \log L(s_{\text{short}}, t)}{\log s_{\text{long}} - \log s_{\text{short}}}, \quad (15)$$

where $s_{\text{short}} < s_{\text{long}}$. This quantity provides a dimensionless, scale-invariant measure of how network connectivity deforms between short and long observation horizons.

When the power-law approximation in Eq. (13) holds locally, the Elastic DCCR coincides with the scaling exponent,

$$\text{Elastic DCCR}(t) \approx \alpha(t), \quad (16)$$

and thus serves as a finite-difference estimate of $\partial \log L / \partial \log s$. Importantly, this interpretation does not require global scale invariance: the Elastic DCCR remains well defined even when the scaling relation holds only approximately or over limited scale ranges.

Sharp temporal variations in the Elastic DCCR indicate local breakdowns of scale invariance and reflect abrupt reconfigurations of network topology. Such events are particularly relevant during periods of market stress, when short-horizon correlations tend to increase rapidly due to liquidity shocks or shifts in risk sentiment, while longer-horizon dependencies adjust more gradually. This scale asymmetry produces transient distortions in the MST geometry, which manifest as spikes or sign reversals in the Elastic DCCR.

By focusing on relative changes across scales rather than absolute levels of connectivity, the Elastic DCCR provides a compact and interpretable diagnostic of multiscale structural instability in correlation networks.

2. Monitoring multiscale network dynamics in financial markets

2.1. Data

We analyze daily closing prices of major equity indices for the G7 countries, China, and Russia. The dataset includes the S&P 500 (United States), S&P/TSX Composite (Canada), CAC 40 (France), DAX (Germany), FTSE MIB (Italy), Nikkei 225 (Japan), FTSE 100 (United Kingdom), Hang Seng Index (China), and the MOEX Russia Index. The sample spans the period from 5 March 2013 to 30 May 2023. All data and code—including automated retrieval from Yahoo Finance—are available at <https://github.com/JoseDLM/Investor-Behavior-and-Multiscale-Cross-Correlations>. Daily prices are converted into logarithmic returns and filtered for heteroskedasticity using a GARCH(1,1) model. Detrended Cross-Correlation Analysis (DCCA) is then applied to the filtered and standardized return series across a range of scales, following the methodology outlined in Section 1. Scale-dependent DCCA coefficients are then transformed into distances using a nonlinear mapping inspired by the construction proposed by Mantegna[24], enabling a geometric representation suitable for Minimum Spanning Tree (MST) construction.

To illustrate the multiscale evolution of cross-market dependencies, we examine the DCCA distances between each index and the S&P 500, taken as a benchmark, over time and across scales.

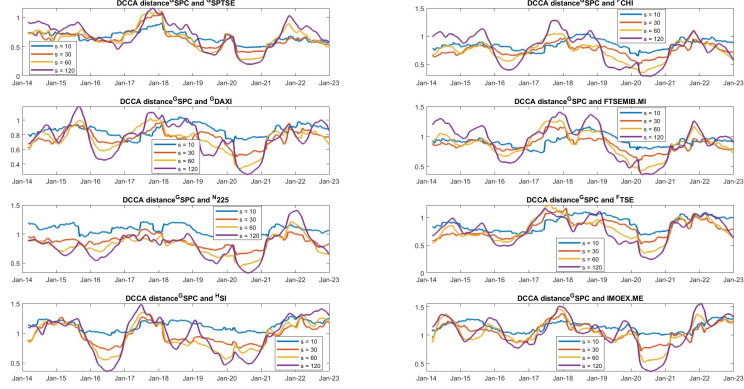


Figure 1: DCCA distances between the S&P 500 and other indices, computed across DCCA scales ranging from $s = 10$ to 120 days using a rolling window of $w = 250$ trading days.

The DCCA distances exhibit clear temporal variation, increasing during periods of market stress and decreasing during stable periods. Short-horizon distances respond more sharply to local fluctuations, reflecting the rapid evolution of short-term dependencies. Longer horizons evolve more slowly and capture persistent structural components of cross-market interactions.

Following the onset of COVID-19, long-horizon distances increase substantially, consistent with scale-dependent reorganization of market structure during the transition from crisis to recovery. Short-horizon distances remain comparatively low throughout the early recovery phase, indicating that short-term co-movements stay elevated even as longer-horizon structure gradually decorrelates.

To track time-varying connectedness, we compute the DCCA distance matrices $d_{\text{DCCA}}^{ij}(s, t)$ using a sliding window of width w with one-day steps. For each $t = 1, \dots, T - w + 1$, distances are estimated from observations in the interval $[t, t + w - 1]$. These distances are then filtered through the MST to obtain the backbone of cross-market interdependencies.

Figures 2 and 3 display kernel density estimates of the MST-filtered DCCA distances at the 1-month and 4-month horizons, respectively. The panels on the right show the first four moments computed over the same rolling window.

These distributional diagnostics complement the Elastic DCCR by revealing higher-order structural changes in the MST backbone that are not captured by average connectivity alone.

At shorter scales, the kurtosis of the MST-filtered distance distribution remains finite, although it increases markedly during turbulent periods. This

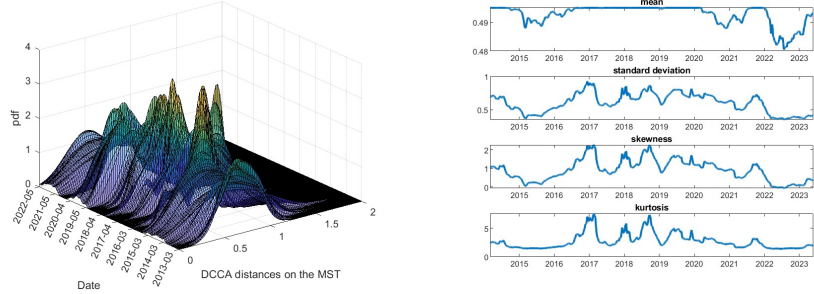


Figure 2: Time evolution of the density of MST-filtered 1-month DCCA distances (left) and the corresponding dynamics of the first four moments (right).

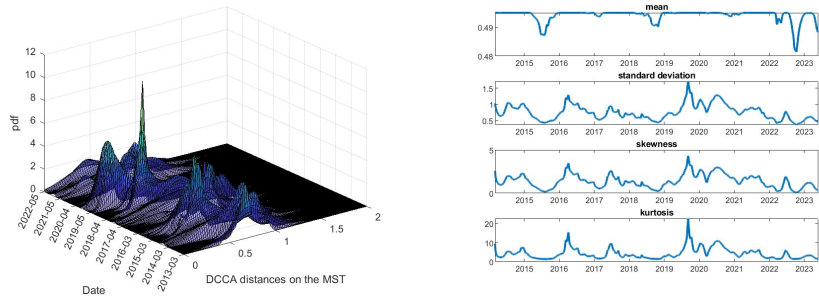


Figure 3: Time evolution of the density of MST-filtered 4-month DCCA distances (left) and the corresponding dynamics of the first four moments (right).

indicates the presence of heavy—but not divergent—tails associated with rapid shifts in short-term cross-market structure. At longer scales, the distributions become more sharply peaked, with occasional episodes of elevated kurtosis reflecting abrupt structural adjustments. In all cases, the fourth moment remains empirically finite, confirming that the distance distributions do not exhibit power-law tails with exponent below 4. The reduced prevalence of extremes at longer scales is consistent with persistent long-range correlation structure.

Periods of instability correspond to elevated uncertainty and rapid adjustments in global risk conditions, producing strong short-term co-movements and scale-dependent distortions of network topology. The multiscale MST representation thus provides a compact and informative view of the temporal evolution of cross-market connectedness.

3. Real versus synthetic networks: a multiscale scaling test

To assess whether the structural changes observed in the correlation-based networks arise from genuine cross-market dependencies rather than from univariate volatility dynamics, we construct a synthetic benchmark based on independent GARCH(1,1) processes. These series reproduce volatility clustering

and heteroskedasticity but contain no cross-correlations by construction. They therefore serve as a baseline for distinguishing multivariate dependence from purely univariate effects. This comparison provides a direct empirical counterpart to the scaling hypothesis introduced in Section 1.3, allowing us to assess when the average MST length follows an approximately local power-law structure and when this structure breaks down.

Our aim is to compare the scale dependence of the average MST length $L(s, t)$ in real and synthetic data, and to identify deviations from power-law behaviour that signal nontrivial multiscale structure. Both systems are analysed using a sliding window of width $w = 250$ trading days, with $t = 1, \dots, T - w + 1$.

Synthetic data. We generate $N = 9$ independent GARCH(1,1) series,

$$r_t = \sigma_t \varepsilon_t, \quad \sigma_t^2 = \omega + \alpha r_{t-1}^2 + \beta \sigma_{t-1}^2,$$

with parameters $\omega = 10^{-6}$, $\alpha = 0.1$, and $\beta = 0.85$, chosen to reflect typical financial-market persistence ($\alpha + \beta = 0.95$) and a reasonable unconditional variance. Each series is initialized with a different random seed, and no cross-correlations are imposed by construction.

Real data. The real dataset consists of daily closing prices for the G7+China+Russia equity indices over 2013–2023, filtered via GARCH(1,1) to remove asset-level heteroskedasticity. The objective is to isolate structural instabilities arising from the cross-correlation network rather than from univariate volatility effects.

We visualize the surface $\log L(s, t)$ over the $(\log s, t)$ plane for scales ranging from 5 to 160 days, logarithmically spaced, to highlight the joint time–scale evolution of network connectivity.

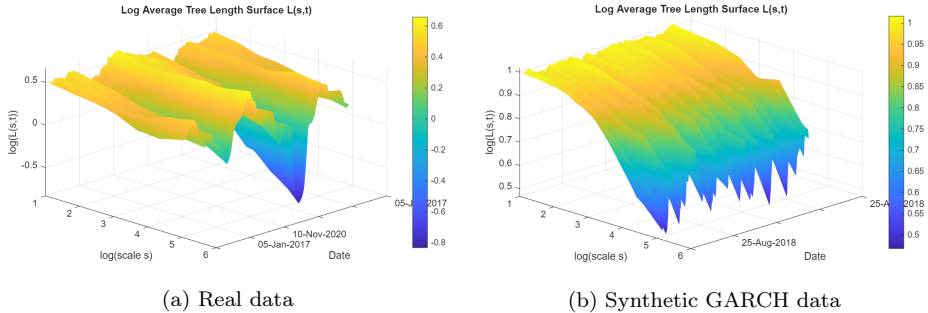
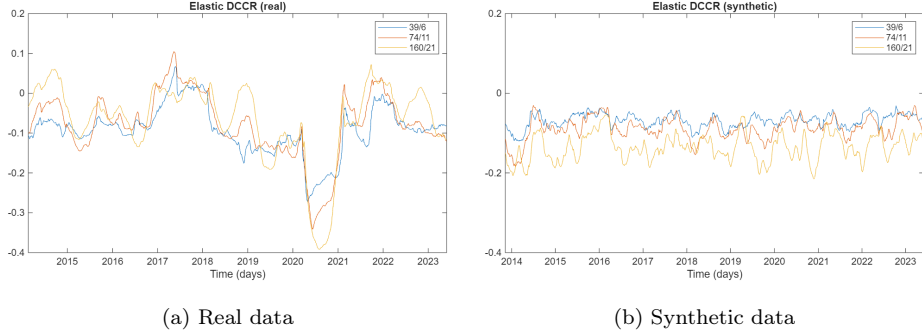


Figure 4: Surfaces of $\log L(s, t)$ over the $(\log s, t)$ plane for real (a) and synthetic (b) data.

Real markets show frequent distortions in the $(\log s, t)$ surface, whereas the synthetic system exhibits a smoother, nearly linear log–log structure. This indicates that the synthetic data are consistent with an approximately local power-law scaling, while real data exhibit scale-dependent disruptions.

The Elastic DCCR is computed for three distinct short- and long-horizon scale pairs, as indicated in the figure legend.

Synthetic data show stable, nearly scale-invariant behavior, while real systems feature intermittent bursts, reflecting multiscale structural shifts in corre-



lation networks. These deviations are consistent with the emergence of collective market dynamics that extend beyond volatility persistence alone.

To further interpret the scale-dependent behavior captured by the Elastic DCCR, we consider additional diagnostic quantities that probe how the average MST length varies with scale. Specifically, examining first- and second-order variations of $\log L(s, t)$ with respect to $\log s$ provides insight into both the local elasticity of network connectivity and the rate at which this elasticity itself changes across horizons. These diagnostics are introduced to complement, rather than replace, the Elastic DCCR.

Local scaling exponent diagnostics. Before examining the local scaling exponent, it is important to note that the interpretation of $\alpha(t)$ differs fundamentally between real and synthetic systems. While a local exponent can be estimated in both cases, in the synthetic GARCH benchmark it reflects a trivial, noise-induced scaling associated with independent series. In contrast, for real markets $\alpha(t)$ provides a diagnostic of nontrivial, time-varying distortions in the multiscale structure of the correlation network.

We estimate the time-varying scaling exponent $\alpha(t)$ via OLS regressions of $\log L(s, t)$ on $\log s$ within moving windows. The resulting goodness of fit, measured by the coefficient of determination R^2 , varies substantially for real data but remains consistently high for the synthetic system:

These results show that real markets frequently depart from linear scale-invariant behavior, while synthetic GARCH series maintain stable power-law structure.

Second-order scaling. To complement the first-order diagnostic based on the local slope, we also examine curvature in the $\log L$ – $\log s$ relation via a local second-order expansion in log–log space,

$$\log L(s, t) = \gamma(t) + \alpha(t) \log s + \beta(t)(\log s)^2. \quad (17)$$

A nonzero $\beta(t)$ signals scale-dependent variations in the effective scaling behavior and departures from simple scale invariance.

Real data display pronounced and time-varying curvature, whereas synthetic data exhibit $\beta(t) \approx 0$, indicating an approximately linear $\log L$ – $\log s$ relation.

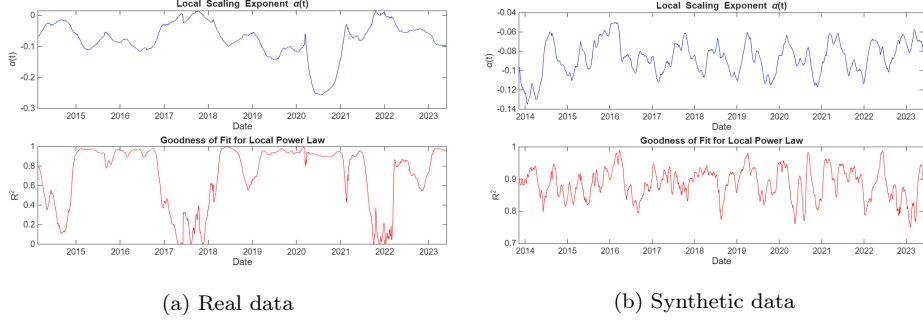


Figure 5: Estimated local scaling exponent $\alpha(t)$ and corresponding R^2 for real (a) and synthetic (b) data.

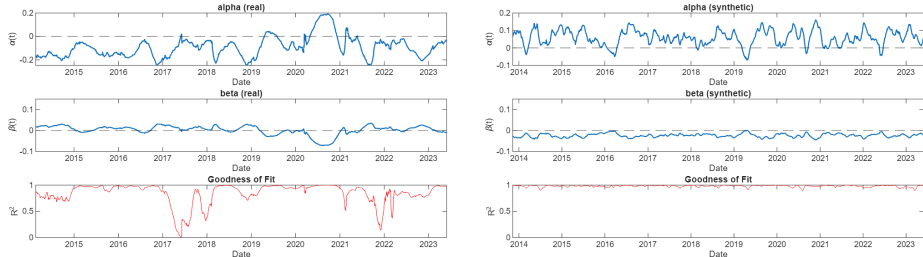


Figure 6: First- and second-order coefficients ($\alpha(t)$, $\beta(t)$) and fit quality (R^2) for real (left) and synthetic (right) data.

The generalized effective exponent,

$$\delta_{\text{eff}}(s, t) = \frac{d \log L(s, t)}{d \log s} = \alpha(t) + 2\beta(t) \log s, \quad (18)$$

highlights scale-dependent shifts in real systems that are not captured by a single, scale-independent exponent.

4. Detecting multiscale network instabilities

We adopt a simple deviation–screening approach to detect abrupt distortions in the multiscale network structure. Let E_t denote the Elastic DCCR, defined using the following two scales,

$s_{\text{long}} = 74$ (approximately 3.5 months) and $s_{\text{short}} = 11$ (approximately 2 weeks). We compute the z -score

$$Z_t = \frac{E_t - \mu_t}{\sigma_t}, \quad (19)$$

where μ_t and σ_t are the 21-day rolling mean and standard deviation of E_t . Observations with $|Z_t| > 2.5$ are classified as *anomalies*. The threshold is used

purely to flag exceptional local deviations without invoking any distributional assumptions.

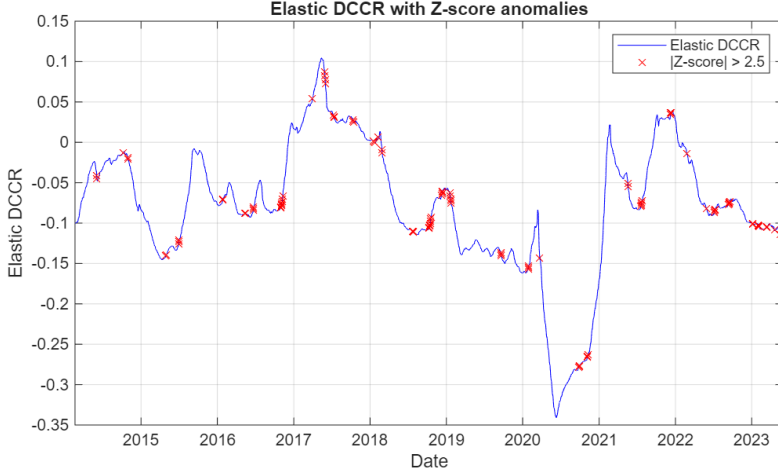


Figure 7: z -score screening of the Elastic DCCR (ratio 74/11); anomalies defined by $|Z_t| > 2.5$.

Points flagged in this manner correspond to short-lived but sharp transitions in the correlation-network topology. This complements volatility-based indicators by capturing structural deviations that are abrupt but not necessarily persistent.

Event matching. To assess the economic relevance of the detected anomalies, we examine clusters of consecutive trading days with $|Z_t| > 2.5$ (bridging weekends) and inspect headline news within a ± 1 -day window.

Sources include international newswires (e.g., Reuters, Yahoo Finance) and policy calendars from major central banks. When several developments coincide with a given cluster, we prioritise internationally relevant events consistent with the global scope of the network.

This retrospective correspondence is judgement-based and hence subject to look-ahead bias. Future work could improve robustness by: (i) restricting the search to a pre-defined calendar of candidate events, and (ii) benchmarking overlaps against randomly shifted event dates.

Event correspondence. As shown in Table 1, the largest Elastic DCCR anomalies align with major global shocks.

The majority of anomaly clusters align with major macro-financial or geopolitical events.

Examples include: Greece’s capital-control announcement (30 June 2015), the U.K. Brexit vote (24 June 2016), the Wuhan lockdown at the onset of COVID-19 (27 January 2020), Pfizer–BioNTech’s vaccine-efficacy announcement (9 November 2020), the Federal Reserve’s “unlimited” QE (23 March 2020), and Gazprom’s suspension of *Nord Stream 1* flows (1 September 2022). Only

Table 1: Selected Elastic DCCR anomaly clusters and corresponding events.

Date range	Max Z	Event type
2015-06-25 – 2015-06-26	2.62	Greek capital controls
2016-06-20 – 2016-06-23	2.84	Brexit referendum
2017-04-03 – 2017-04-04	2.75	Article 50 negotiations
2020-01-27 – 2020-01-28	2.58	Wuhan lockdown
2020-11-09 – 2020-11-10	2.59	Pfizer–BioNTech vaccine

a few clusters lack an identifiable contemporaneous driver, indicating that the Elastic DCCR predominantly captures economically meaningful structural shifts rather than statistical artefacts.

Sign information. The sign of the deviation provides additional interpretation. **Positive** spikes ($Z_t > 0$) typically coincide with periods of stress and risk-off compression in cross-market dependencies. **Negative** spikes ($Z_t < 0$) tend to follow strong stabilisation signals (e.g., quantitative-easing announcements or vaccine breakthroughs) and reflect a rapid re-differentiation of correlations across scales. Although exceptions occur (e.g., the *Nord Stream 1* shutdown yields a negative spike), the overall pattern supports interpreting Z_t as a proxy for the balance between correlation compression and relaxation.

These episodes correspond to well-known global shocks associated with abrupt reconfigurations of cross-market dependencies.

Interpretation. Although individual return series exhibit comparable long-range memory properties, the Elastic DCCR reveals scale-dependent reconfiguration of the correlation network.

These deformations correspond to system-level adjustments triggered by macroeconomic shocks, suggesting that the observed instabilities arise from evolving interdependencies rather than marginal volatility dynamics.

The analysis of $L(s, t)$ across scales yields two main insights:

1. **Local scaling.** Log-log plots of $L(s, t)$ versus s are approximately linear over limited scale ranges at each time point. This motivates the use of a time-varying scaling exponent $\alpha(t)$ as a diagnostic of local structural complexity.
2. **Deviation from perfect scaling.** A curvature-based diagnostic indicates that the mean curvature of the log-log profiles is nonzero. Thus, although the relationship is locally linear, the system does not follow an exact power law globally. The persistent curvature is consistent with multiscale, and potentially multifractal, organisation of the correlation network.

5. Comparison with the DCCA–GARCH approach of Diebold et al.

We compare our multiscale network methodology with the connectedness framework of Diebold et al. [22, 29]. Their approach measures directional and

system-wide connectedness using generalized forecast-error variance decompositions (GVDs) from vector autoregressions (VARs). In this setting, connectedness reflects the extent to which shocks to one variable contribute to the forecast-error variance of another, thereby quantifying the propagation channels of system-wide risk.

Let d_{ij}^H denote the H -step-ahead GVD component that attributes the forecast-error variance of variable i to shocks in variable j ($i \neq j$). The $N \times N$ connectedness table is then constructed from these non-own variance decompositions, with row and column sums representing directional “from”, “to”, and “net” connectedness. The framework uses the generalized variance-decomposition approach of Koop et al. [30] and Pesaran and Shin [31], which avoids the ordering dependence inherent in Cholesky-based orthogonalization and preserves the empirical correlation structure of shocks.

Following Refs. [22, 29], we estimate a rolling VAR with window width $w = 250$ trading days to obtain time-varying total connectedness. Figure 8 shows the resulting series using the same dataset as in previous sections. A full directional connectedness table is provided in Appendix 6.

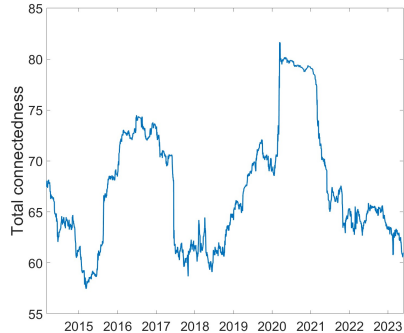


Figure 8: Time-varying total connectedness in the sense of Diebold et al., using a rolling window of $w = 250$ days.

The Diebold et al. total connectedness measure exhibits a strong empirical correlation with the dominant eigenvalue of the DCCA-based adjacency matrix (Pearson correlation 0.81 for $w = 250$), with similarly strong correlations observed for other window lengths.

We compute “to”, “from”, and “net” directional components for completeness, and the code replicating all results is provided in the project repository.

Conceptual differences. Our approach differs from the Diebold et al. framework in two key respects:

1. **Cross-correlation metric.** We transform scale-dependent DCCA coefficients into a geometric distance, enabling the construction and monitoring of minimum spanning trees across scales. This provides a sparse, interpretable representation of evolving cross-market structure.

2. **Relaxation of covariance-stationarity.** The DCCA-based methodology does not require covariance stationarity or VAR specifications, allowing it to capture long-memory effects, slowly varying dependencies, and multiscale structure that may be difficult to accommodate within variance-decomposition frameworks.

Thus, while the Diebold et al. measure offers a VAR-based description of shock propagation, our framework provides a multiscale, topology-oriented view of connectedness that remains applicable in the presence of long-range dependence and structural nonstationarity.

6. Conclusions

We introduce a multiscale framework for detecting structural transitions in complex systems by analysing the evolution of cross-correlation networks. The approach combines Detrended Cross-Correlation Analysis (DCCA) with Minimum Spanning Tree (MST) filtering to obtain a sparse, multiscale representation of interdependencies. Its core component, the Elastic Detrended Cross-Correlation Ratio (Elastic DCCR), provides a dimensionless measure of how network topology responds to changes in observational scale, thereby capturing local departures from scale-invariant behaviour.

Applied to global equity indices, the method identifies clear episodes of topological reorganisation coinciding with major financial disruptions. These shifts manifest as short-horizon correlation compression and long-horizon structural fragmentation, suggesting changes in the underlying coordination of market components. The Elastic DCCR effectively isolates these transitions, revealing multiscale adjustments that are not visible in single-scale or static measures of dependence.

Because the framework relies solely on scale-dependent correlations and does not require covariance stationarity, it is applicable to a broad class of systems characterised by long-range dependence or nonstationary interactions. Potential applications include climate networks, neuronal or biological systems, and engineered infrastructures. In this sense, the Elastic DCCR provides a general and interpretable tool for monitoring multiscale sensitivity to structural change and identifying emerging instability regimes in complex interconnected systems.

Research perspectives and extensions

Scale-invariant cross-correlation under heterogeneous long-range dependence

A natural extension of this work concerns the behaviour of DCCA-based correlation measures when the underlying time series exhibit heterogeneous scaling properties. In many systems, the Hurst exponents H_x and H_y of two series differ substantially, reflecting asymmetric persistence, multifractality, or heterogeneous long-range memory. Under such conditions, the standard DCCA normalization may no longer guarantee boundedness or approximate scale invariance of $\rho_{\text{DCCA}}(s)$, particularly when the associated fluctuation functions grow at different rates.

One possible direction is a scaling-adjusted normalization that weights the DFA fluctuation functions according to their relative scaling exponents,

$$\tilde{\rho}_{\text{DCCA}}(s) = \frac{F_{\text{DCCA}}^2(s)}{F_{\text{DFA},x}(s)^\alpha F_{\text{DFA},y}(s)^{1-\alpha}}, \quad (20)$$

with

$$\alpha = \frac{H_y}{H_x + H_y}. \quad (21)$$

Assuming the scaling relations

$$F_{\text{DFA},x}(s) \sim s^{H_x}, \quad F_{\text{DFA},y}(s) \sim s^{H_y}, \quad F_{\text{DCCA}}^2(s) \sim s^{2H_{xy}}, \quad (22)$$

the generalized coefficient behaves as

$$\tilde{\rho}_{\text{DCCA}}(s) \sim s^{2H_{xy} - (\alpha H_x + (1-\alpha) H_y)}. \quad (23)$$

Choosing $\alpha = H_y/(H_x + H_y)$ yields an exponent that coincides with H_{xy} under idealized conditions, thereby attenuating spurious scale dependence.

While such an adjustment does not ensure strict boundedness in $[-1, 1]$, it may improve robustness when analysing systems with heterogeneous long-range dependence. For distance-based network applications, the resulting coefficient could be further transformed or clipped to maintain metric compatibility.

Eigenvalue-based stability and multiscale network sensitivity

The eigenvalue spectrum of a scale-dependent adjacency matrix provides an additional diagnostic of structural stability in evolving networks. In many dynamical systems, the dominant eigenvalue governs the sensitivity of collective modes to perturbations and the onset of instability [32]. A large leading eigenvalue indicates strong effective coupling, favouring rapid propagation of shocks and reduced resilience.

In the present context, the dominant eigenvalue of the DCCA-based adjacency matrix, or of its MST-filtered counterpart, offers a complementary measure of system-wide coherence. A systematic comparison between the Elastic DCCR and the temporal evolution of the leading eigenvalue may reveal whether breakdowns of approximate scale-invariance coincide with increased spectral concentration. Such an analysis could clarify how multiscale deformation of network topology is linked to the emergence of collective instability modes.

Future work may therefore explore joint diagnostics combining: (i) scale-dependent topological sensitivity (Elastic DCCR), and (ii) spectral stability indicators derived from the adjacency matrix. This pairing has the potential to identify early-warning signatures of instability in a wide class of multiscale networks.

Connection between scaling behaviour and cointegration

A further research direction concerns the potential connection between the scaling exponent $\alpha(t)$ —and hence the Elastic DCCR—and the concept of cointegration. If two price series are cointegrated, their log levels share a common stochastic trend, while deviations from equilibrium remain stationary. Within the DCCA–MST framework, such long-run co-movement is expected to manifest as persistently high $\rho_{\text{DCCA}}(s)$ at large scales s , leading to small DCCA distances

$$d_{ij}(s) = \sqrt{2(1 - \rho_{ij,\text{DCCA}}(s))}.$$

Under an empirical scaling relation of the form $L(s, t) \propto s^{\alpha(t)}$, this behaviour is consistent with values of $\alpha(t)$ that are close to zero or negative, indicating that distances do not increase with scale. Conversely, positive values of $\alpha(t)$ reflect dominance of short-term co-movement and are consistent with the absence, or breakdown, of stable cointegrating relationships.

From this perspective, $\alpha(t)$ and the Elastic DCCR may be viewed as non-parametric, scale-dependent diagnostics of long-run co-movement. Persistent near-zero or negative values would be associated with stable long-run linkages, whereas positive or highly volatile values may signal fragmentation of equilibrium relationships, as often observed during crisis periods. Exploring this connection could provide a multiscale interpretation of cointegration and help bridge traditional error-correction models with geometric network representations.

Appendix A: Statistics of interest

Table A1 reports descriptive statistics for the observed equity-index return series, including annualised mean and volatility, skewness, kurtosis, autocorrelation at various lags, and autocorrelation of squared returns.

Stat\Tickers	GSPC	GSPTSE	FCHI	GDAXI	FTSEMIB.MI	N225	FTSE	HSI	IMOEX.ME
Ann. mean	0.10	0.04	0.06	0.07	0.05	0.09	0.02	-0.02	0.06
Ann. vol	0.18	0.15	0.19	0.19	0.23	0.20	0.16	0.20	0.22
Skewness	-0.82	-1.66	-0.81	-0.58	-1.41	-0.19	-0.88	0.04	-2.25
Kurtosis	19.24	45.30	13.49	12.85	19.01	7.77	15.94	6.90	53.33
AC 1d	-0.14***	-0.09***	-0.00	-0.01	-0.06***	-0.02	-0.00	0.01	0.09***
AC 5d	0.05***	0.04***	0.00	0.01	0.01***	-0.01***	0.02	-0.03	-0.02***
AC 10d	-0.06***	-0.03***	-0.03***	-0.04***	-0.01***	-0.02***	-0.00***	-0.00	-0.04***
AC 20d	-0.02***	0.00***	0.02**	0.03***	-0.00**	-0.01***	0.04***	0.05*	-0.02***
AC sq. ret 1d	0.48***	0.43***	0.11***	0.06***	0.15***	0.21***	0.17***	0.28***	0.68***
AC sq. ret 5d	0.32***	0.28***	0.12***	0.08***	0.06***	0.08***	0.11***	0.13***	0.02***
AC sq. ret 10d	0.24***	0.14***	0.11***	0.09***	0.05***	0.14***	0.14***	0.09***	0.01***
AC sq. ret 20d	0.11***	0.06***	0.05***	0.07***	0.01***	0.03***	0.09***	0.06***	0.02***

Notes: *, **, and *** denote significance at the 5%, 1%, and 0.1% levels, respectively.

Table A1: Summary statistics for the equity-index return series.

Tables A2 and A3 present full-sample DCCA coefficients at the 1- and 4-month time scales.

DCCA coefficients ($s = 1$ month)								
	US	CA	FR	DE	IT	JP	UK	CN
CA	0.8280							
FR	0.7336	0.7491						
DE	0.7350	0.7269	0.9416					
IT	0.6543	0.6786	0.8995	0.8697				
JP	0.6050	0.5814	0.6624	0.6429	0.5874			
UK	0.6960	0.7548	0.8667	0.8215	0.7727	0.6054		
CN	0.4948	0.4886	0.5283	0.5085	0.4645	0.5446	0.5302	
RU	0.3948	0.4495	0.4649	0.4677	0.4328	0.3520	0.4584	0.3497

Table A2: Full-sample DCCA coefficients at the 1-month time scale.

DCCA coefficients ($s = 4$ months)								
	US	CA	FR	DE	IT	JP	UK	CN
CA	0.8584							
FR	0.7972	0.7986						
DE	0.7913	0.7745	0.9321					
IT	0.6950	0.7287	0.9128	0.8625				
JP	0.7212	0.6405	0.7217	0.7567	0.6484			
UK	0.7869	0.8280	0.8734	0.8429	0.7786	0.6742		
CN	0.4972	0.4731	0.5104	0.4895	0.4717	0.4481	0.5716	
RU	0.4788	0.4997	0.5387	0.5514	0.5290	0.4510	0.5257	0.3614

Table A3: Full-sample DCCA coefficients at the 4-month time scale.

Appendix B: Diebold et al. measure of connectedness

Table B1 reports the Diebold–Yilmaz connectedness measures computed for the dataset.

References

- [1] F. X. Diebold, K. Yilmaz, Measuring financial asset return and volatility spillovers, with application to global equity markets, *Economics Letters* 124 (1) (2009) 24–28.
- [2] J. Baruník, T. Krehlik, Measuring the connectedness between financial markets: a dynamic network approach, *Journal of Financial Economics* 130 (2) (2018) 256–280.
- [3] R. Cont, Empirical properties of asset returns: stylized facts and statistical issues, *Quantitative Finance* 1 (2) (2001) 223–236.
- [4] M. Kritzman, S. Page, The efficient frontier: A return-to-risk measure, *The Journal of Portfolio Management* 29 (4) (2003) 40–50.

	GSPC	GSPTSE	FCHI	GDAXI	FTSE.MIB	N225	FTSE	HSI	IMOEX.ME	From
GSPC	27.59	18.18	10.89	10.56	8.83	6.93	9.93	4.28	2.76	72.40
GSPTSE	18.34	27.39	18.86	10.02	9.41	4.71	11.75	3.87	3.60	72.60
FCHI	8.30	8.74	20.97	18.33	16.40	4.67	15.29	3.68	3.59	79.02
GDAXI	8.46	8.42	18.92	21.83	15.99	4.82	14.45	3.48	3.58	78.16
FTSE.MIB	7.82	8.53	17.98	16.96	23.98	4.42	13.53	3.19	3.53	76.01
N225	5.69	5.52	7.42	6.43	5.52	51.29	7.39	8.55	2.15	48.70
FTSE	8.37	10.28	16.76	15.35	13.58	4.18	23.28	4.11	4.04	76.71
HSI	3.99	5.25	7.60	6.80	5.62	6.37	8.43	52.54	3.35	47.45
IMOEX.ME	4.63	6.52	8.40	8.08	7.47	2.71	8.56	3.28	50.31	49.68
To	65.64	71.47	98.88	92.56	82.86	38.85	89.37	34.47	26.64	66.75
Net	-6.76	-1.13	19.85	14.39	6.85	-9.84	12.65	-12.97	-23.03	0

Table B1: Diebold–Yilmaz connectedness table for the full sample.

- [5] A. Serletis, A. Kanas, Correlations and volatility spillovers among international stock markets, *Journal of International Financial Markets, Institutions and Money* 12 (1) (2002) 1–23.
- [6] H. Markowitz, Portfolio selection, *The Journal of Finance* 7 (1) (1952) 77–91.
- [7] L. Bauwens, J. V. K. Rombouts, Multivariate volatility models: A survey, *Journal of Economic Surveys* 23 (3) (2009) 517–556.
- [8] R. F. Engle, B. Kelly, Dynamic conditional correlation: A simple class of multivariate garch models, *Journal of Business & Economic Statistics* 30 (3) (2012) 335–349.
- [9] Z. Zheng, B. Podobnik, L. Feng, B. Li, Changes in cross-correlations as an indicator for systemic risk, *Scientific Report* 2 (2012) 1–8. doi:10.1038/srep00888.
- [10] D. Sornette, *Why Stock Markets Crash: Critical Events in Complex Financial Systems*, Princeton University Press, 2003.
- [11] L. Kristoufek, Fractal markets hypothesis and the global financial crisis: Scaling, investment horizons and liquidity, *Advances in Complex Systems* 15 (2012) 1250065. doi:10.1142/S0219525912500658.
- [12] L. Kristoufek, Fractal markets hypothesis and the global financial crisis: Wavelet power evidence, *Scientific Reports* 3 (2013) 1–7. doi:10.1038/srep02857.
- [13] E. Peters, *Fractal market analysis: Applying chaos theory to investment and analysis*, John Wiley & Sons, Inc., 1994.
- [14] T. Adrian, M. K. Brunnermeier, Covar, *American Economic Review* 106 (7) (2016) 1705–1741.
- [15] F. X. Diebold, K. Yilmaz, E. Kocenda, The network topology of variance decompositions: Measuring the connectedness of financial firms, *Journal of Econometrics* 182 (1) (2012) 119–134.

- [16] K. J. Forbes, R. Rigobon, No contagion, only interdependence: Measuring stock market comovements, *Journal of Finance* 57 (5) (2002) 2223–2261.
- [17] B. Podobnik, H. Stanley, Detrended cross-correlation analysis: A new method for analyzing two non-stationary time series, *Physical Reviews Letters* 100 (2008) 084102. [doi:10.1103/PhysRevLett.100.084102](https://doi.org/10.1103/PhysRevLett.100.084102).
- [18] W.-X. Zhou, D. Sornette, The dependence structure of financial assets in bull and bear markets, *Quantitative Finance* 3 (3) (2003) 226–233. [doi:10.1080/1469768031000085331](https://doi.org/10.1080/1469768031000085331).
- [19] A. Bunde, S. Havlin, J. F. S. M. da Silva, H. E. Stanley, Long-term memory in finance: Evidence from multifractality and power-law cross-correlations, *European Physical Journal B* 48 (4) (2005) 467–474. [doi:10.1140/epjb/e20050019](https://doi.org/10.1140/epjb/e20050019).
- [20] L. Yang, C.-T. Hsu, Cross-correlation analysis of two financial time series using dcca, *Physica A: Statistical Mechanics and its Applications* 391 (3) (2012) 931–939. [doi:10.1016/j.physa.2011.10.051](https://doi.org/10.1016/j.physa.2011.10.051).
- [21] L. Wang, Y. Zhang, Cross-correlation analysis of stock returns with detrended fluctuation analysis and detrended cross-correlation analysis, *Chaos, Solitons & Fractals* 74 (2015) 160–171. [doi:10.1016/j.chaos.2015.02.010](https://doi.org/10.1016/j.chaos.2015.02.010).
- [22] F. X. Diebold, K. Yilmaz, J. Barunik, E. Kocenda, A. Sensoy, On the network topology of variance decompositions: Measuring the connectedness of financial firms, *Journal of Econometrics* 182 (2014) 119–134. [doi:10.1016/j.jeconom.2014.04.012](https://doi.org/10.1016/j.jeconom.2014.04.012).
- [23] C. K. Peng, S. V. Buldyrev, S. Havlin, M. Simons, H. E. Stanley, A. L. Goldberger, Mosaic organization of DNA nucleotides, *Physical Review E: Statistical Physics, Plasmas, Fluids, and Related Interdisciplinary Topics* 49 (2) (1994) 1685–1689. [doi:10.1103/physreve.49.1685](https://doi.org/10.1103/physreve.49.1685).
- [24] R. N. Mantegna, Hierarchical structure in financial markets, *The European Physical Journal B* 11 (1999) 193–197. [doi:10.1007/s100510050929](https://doi.org/10.1007/s100510050929).
- [25] J. P. Onnela, A. Chakraborti, K. Kaski, J. Kertész, A. Kanto, Dynamics of market correlations: Taxonomy and portfolio analysis, *Physical Review E* 68 (2003) 056110. [doi:10.1103/PhysRevE.68.056110](https://doi.org/10.1103/PhysRevE.68.056110).
- [26] M. Tumminello, T. Aste, T. Di Matteo, R. N. Mantegna, A tool for filtering information in complex systems, *Proceedings of the National Academy of Sciences* 102 (30) (2005) 10421–10426. [doi:10.1073/pnas.0500298102](https://doi.org/10.1073/pnas.0500298102).
- [27] G. Bonanno, F. Lillo, R. N. Mantegna, Topology of correlation-based minimal spanning trees in real and model markets, *Physical Review E* 68 (4) (2003) 046130. [doi:10.1103/PhysRevE.68.046130](https://doi.org/10.1103/PhysRevE.68.046130).

- [28] J. B. Kruskal, On the shortest spanning subtree of a graph and the traveling salesman problem, *Proceedings of the American Mathematical Society* 7 (1) (1956) 48–50. doi:10.2307/2033241.
- [29] F. X. Diebold, Yilmaz, Reprint of: On the network topology of variance decompositions: Measuring the connectedness of financial firms, *Journal of Econometrics* 234 (2023) 70–90. doi:10.1016/j.jeconom.2023.03.003.
- [30] G. Koop, M. H. Pesaran, S. M. Potter, Impulse response analysis in non-linear multivariate models, *Journal of Econometrics* 74 (1) (1996) 119–147.
- [31] H. H. Pesaran, Y. Shin, Generalized impulse response analysis in linear multivariate models, *Economics Letters* 58 (1) (1998) 17–29.
- [32] C. Sarkar, S. Jalan, Spectral properties of complex networks, *Chaos* 21 (2) (2011) 025106. doi:10.1063/1.5040897.

Author contributions

All authors contributed equally to this work. M. D., G. K., L. L. and J. DLM. participated in the study design, data analysis, interpretation and manuscript preparation. All authors approved the final version.

Additional information

Competing interests: The authors declare no competing interests.